Available online at www.sciencedirect.com

jmr&t Journal of Materials Research and Technology

journal homepage: www.elsevier.com/locate/jmrt

Original Article

Study on two eco-friendly surface treatments on *Luffa cylindrica* for development of reinforcement and processing materials

Maria-Belen Martinez-Pavetti [a,b], *Lucas Medina* [a], *Magdalena Espínola* [a], *Magna Monteiro* [a,*]

[a] *Bio & Materials Laboratory, Polytechnic School, National University of Asuncion, San Lorenzo, P.O.Box – 2111, SL, Paraguay*

[b] *Research Center in Mathematics, Asuncion, Paraguay*

ARTICLE INFO

Article history:
Received 6 May 2021
Accepted 28 July 2021
Available online 3 August 2021

Keywords:
Characterization
Luffa cylindrica
Natural fibers
Surface treatments

ABSTRACT

The development of new materials or the improvement of their mechanical properties is a constant challenge in science. Numerous researchers have increasingly concentrated efforts to obtain new and more environmentally friendly materials using natural fibers, which, to be used in engineering applications, usually have to undergo thermochemical treatments. This work aims to evaluate and compare the effects of two low-cost and low-impact thermochemical treatments on *Luffa cylindrica* (LC) fibers to verify why different mechanical strengths are reached when applying these variations in the production of compressed earth blocks. Samples of LC fibers in three conditions were studied, LC fibers without treatment or natural LC fibers (LN), fibers treated with boiled water (LW) and fibers treated with sodium hydroxide (LS). Samples were analyzed by SEM/EDS to verify surface changes and chemical composition. The lignin, hemicellulose, amorphous and crystalline cellulose structures were determined by FTIR. XRD technique was used to determine the amorphous and crystalline phases, as well as the crystallinity index and the crystallite size. Both treatments decreased the crystallinity index, but the sodium hydroxide treatment has given a crystallinity higher than that of the water treatment. However, the water treatment cannot be ignored. Perhaps more convenient results can be achieved by varying the water treatment time.

1. Introduction

The pursuit of a more environmentally friendly society promotes substantial research to develop new materials using natural fibers. Some natural fibers as sugar cane bagasse [1], jute [2–5], sisal and other fibers are being studied for engineering purposes and novel applications for their availability, ease of processing, and appealing properties [6].

In this context, natural sponges, in particular *Luffa cylindrica* (LC), are rising as attractive candidates for natural reinforcement of composites [7–13] and transformation materials

* Corresponding author.
E-mail address: mmonteiro@pol.una.py (M. Monteiro).
https://doi.org/10.1016/j.jmrt.2021.07.141

for environmental improvement applications such as wastewater remediation [14,15]. These sponges are attractive because they have good properties in their natural state and undergo advantageous surface changes or improve their physicochemical and mechanical characteristics when subjected to surface treatments [8].

The effect of the LC fibers as aggregates in different matrices has been studied in the composite materials field. Martinez-Barrera et al. [7] added LC fibers to a polymeric concrete matrix and reported that the fracture strain increased despite the decrease in compressive and flexural strength. Dias et al. [8] studied natural LC fibers and fibers submitted to acid, acid/basic, basic/acid and basic thermochemical treatment. They reported that the sample presenting a higher mass loss percentage was treated with a basic/acid solution and that there is higher crystallinity in this sample, contrary to the effect of the alkaline treatment, which increases the amorphous cellulose content. Colorado et al. [11] manufactured cement composites using LC fibers treated with acid and alkaline processes, and they observed good matrix-fibers adhesion. Mota [12] studied a polymeric composite reinforced with LC fibers treated with boiled water and reported that although matrix-fibers adhesion was low, fibers reduced cracks propagation. Finally, an interesting review of developments on natural luffa fibers composites can be seen in [16].

On the other hand, results regarding water treatment applications are encouraging as well. Kesraoui et al. [17] used LC to obtain hybrid materials with metallic oxides as ZnO and Al_2O_3, to be applied to water decontamination with anionic and cationic dyes from the textile industry, reporting that the synthesis was successful and that the LC-ZnO material displayed more positive results than LC-Al_2O_3 material. Liatsou et al. [18] studied LC fibers as raw material to produce oxidized biochar fibers for the adsorption of tetravalent thorium ions, Th(IV), using batch system equilibrium. The oxidized biochar fibers showed an excellent adsorption capacity for Th(IV) due to their large external surface, provided by microchannels and surface functional groups (carboxylic groups), increasing the chemical affinity for acid media cationic species. Ad et al. [14] studied the adsorption of nickel ions, Ni(II), from saline solution using LC as adsorbent through different experiments varying initial pH, initial Ni(II) concentration, and salt concentration. They demonstrated that the optimum medium for Ni(II) adsorption was with pH 6, contact time at 180 min, and an initial metal concentration of 10 mg L^{-1}. Khadira et al. [19] showed that LC reinforced with polypyrrole is a low-cost new composite that efficiently removes ibuprofen from aqueous media. The removal results proved that *Luffa cylindrica* with polypyrrole was more effective than raw LC.

Li and Zhang [20] reported that two carbon forms exist in activated carbon fibers (ACF), amorphous and graphite carbon. The amorphous carbon can be free-activated carbon on the ACF surface and non-graphitizable carbon crystallite. LC could also be used to obtain activated carbon. It is possible that the acid solution removes lignin and hemicellulose phases from *luffa,* which favors the amorphous carbon phase formation.

In previous works of this group, on the manufacture of compressed earth blocks (CEB), a block with lower mechanical performance and higher weight than expected was obtained, in comparison with typical commercial blocks. Natural *Luffa cylindrica* was added as filler for best performance, but the results were not significantly different. Therefore, this work studied and compared two thermochemical treatments of low cost and low impact, with boiled water and sodium hydroxide, applicable to *Luffa cylindrica* fibers to be used as fillers of CEB in order to improve its performance. The natural and treated LC samples were analyzed by scanning electron microscopy (SEM) coupled with energy dispersive spectroscopic (EDS) to verify surface and chemical composition changes. The X-ray diffraction (XRD) technique was used to determine the amorphous and crystalline phases, as well as the crystallinity index and crystallite size. The structures of lignin, hemicellulose, amorphous cellulose, and crystalline cellulose type were determined by Fourier-transform infrared spectroscopy (FTIR). These analyzes allow a better understanding of the differences between the mechanical performance results of the LC-reinforced CEB obtained with each treatment. In this work, only the treatment studies are presented.

2. Methodology

Luffa sponges were purchased from local producers (Central, Paraguay). Before characterization, the sponges were cleaned with double distillate water after manually removing skin and seeds.

Three different states of LC fibers were studied, which are natural LC fibers (LN) without treatment, LC fibers submitted to boiled water treatment (LW) without any chemical products, and LC fibers submitted to sodium hydroxide treatment (LS). For the sodium hydroxide treatment, a solution (0.1 mol/L) of commercial sodium hydroxide dissolved in double distillate water was prepared. For both treatments, LC pieces were introduced in a vessel containing the treatment medium and heated until boiling point, in which they remained for 20 min. The mixture was continuously stirred throughout this process. Both samples were washed with double distillate water after treatment. The treated samples were then dried in an oven at 50 °C and weighed until constant weight. The treatment procedures were adapted from [8,11,12].

The surface structure and the chemical composition of the samples were examined by SEM/EDS (EVO15, Zeiss Company, Germany), the samples were sputter-coated with a thin gold film. FTIR spectrometer Nicolet iS5 (Thermo Scientific, USA) was used to identify the vibrational of functional groups, preparing the samples as KBr pellets and recording spectra in the range between 400 and 4000 cm^{-1}, with a resolution of 4 cm^{-1} with 128 scans. XRD patterns of the samples were collected using an X'pert3 Powder diffractometer (Malvern Panalytical, Netherlands) with a CuKα source, using 40 kV and 35 mA, 2θ range of 10–90°, the step size was 0.01° and the time step was 0.5 s.

Crystalline phase percentages CP_{XRD} were determined from the relation between crystalline and amorphous regions, obtained from XRD analysis (Eq. (1)) [21]:

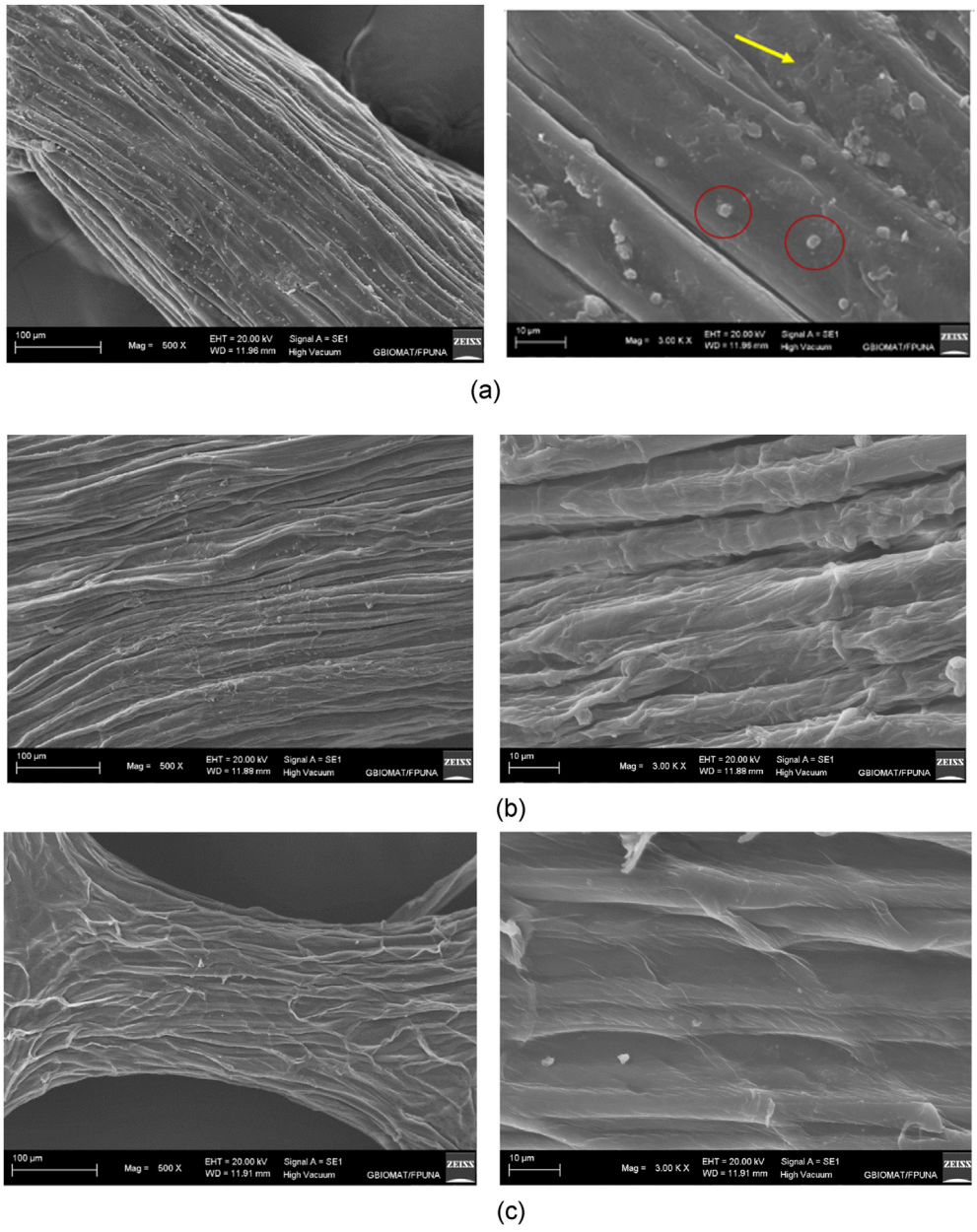

Fig. 1 – SEM micrographs of the *Luffa cylindrica* fibers (a) untreated (LN) and submitted to thermochemical treatments of (b) boiled water (LW) and (c) sodium hydroxide solution (LS). Red circles– calcium particles, and yellow arrow – waxy and gummy substances.

$$CP_{XRD} = \frac{(I_{002} - I_{am})}{I_{002}} \times 100\% \quad (1)$$

In equation (1), CP_{XRD} represents the relative degree of crystallinity, I_{002} is the area of the maximum intensity (a.u.) of the (002) lattice diffraction between 21 and 24° and the I_{am} is the amorphous area of diffraction (a.u.) at $2\theta = 18°$.

The Scherrer equation (Eq. (2)) was used to calculate the crystallite size D of LN, LW and LS samples.

$$D = \frac{K \times \lambda}{\beta \times \cos\theta} \text{ (nm)} \quad (2)$$

In equation (2), $K = 0.9$ is the Scherrer constant; $\lambda = 0.15406$ nm is the wavelength of the X-ray source; β is the full width at half maximum (FWHM) in radians, and θ is the Bragg angle in radians or degrees. The fitting deconvolution was performed by subtracting the background and applying the Gaussian nonlinear curve as the shape function (Eq. (3)) using the Origin Pro 2020 software.

$$y = y_0 + \frac{A}{\beta.\sqrt{\left(\frac{\pi}{4\ln(2)}\right)}} \times exp\left(-4\ln(2)\frac{(x - x_c)^2}{\beta^2}\right) \quad (3)$$

In equation (3), A > 0 = area above the curve; y_0 = base; x_c = center; β = FWHM of each peak.

The results obtained were compared with the pressed earth blocks' mechanical performance to identify the most adequate treatment and the lowest cost.

3. Results and discussions

Luffa sponge has an interlocking arrangement with strongly united interconnections as a scaffold structure. It has a geometrically complex configuration composed of fibers with different lengths, orientations and diameters, depending on the region. These features lead to an anisotropic structure of great interest for many applications.

3.1. SEM analysis

Fig. 1 shows the morphology of treated and untreated luffa fibers obtained by SEM analysis. Fig. 1a shows that natural *luffa* has small embedded particles (red circles) and also membranes (yellow arrow) which could be the waxy and gummy substances, apparently distributed throughout the surface of the sample [22,23].

In Fig. 1b, it is possible to appreciate the micrographs of the LW sample. The surface of the LW sample presents a topography cleaner and smoother than that of LN due to the removal of the lignin and hemicellulose, becoming possible to more sharply see the microfibers in the same direction of the luffa fiber. Moreover, it is yet possible to see some remaining particles embedded. According to Fig. 2, these encrusted particles present an intense concentration of calcium which could be calcium carbonate. It is probable that the LC has the natural ability to form calcium compounds precipitates on its surface. This property could make LC considered a promising raw material in materials processing for biomedical and environmental applications.

Fig. 1c presents the surface morphology of the LS sample, which shows an even smoother surface morphology, with fewer striations and a more polished appearance. The LS sample does not have a surface composed of a bundle of individual fibers, as observed in the LW sample possibly due to the swelling caused by water absorption. Instead, the surface of the LS sample looks like groups of coalescent fibers. Besides, the treatment conditions used in this work (time and concentration of the solution) did not cause severe damage to the fibers, since their interior is not exposed. Therefore, this treatment with NaOH, although more severe than the treatment with water, did not damage the fiber integrity.

Therefore, this treatment with NaOH, although more severe than the treatment with water, produced convenient surface changes without damaging the fiber integrity.

The results obtained by SEM and EDS, image and chemical composition, are shown in Fig. 1 and Table 1, respectively. The calcium content decreases with the treatments, and the highest reduction is observed for the sample treated with sodium hydroxide. This is corroborated with the SEM results, Fig. 1c, since the LS sample has a smoother surface morphology that looks more polished and has fewer striations.

3.2. FTIR analysis

Fig. 3 presents the FTIR spectra with the vibrational of functional groups of the LN, LW, and LS samples. All bands found have been reported in the literature.

According to Fig. 3, it can be seen that the most significant changes are found around the 3402, 2920, 1735, 1640, and 1047 cm^{-1} bands. The bands between 3600 and 3000 cm^{-1} correspond to the hydroxyl OH of the −OH group linked by hydrogen. These bands might correspond to either cellulose I or cellulose II [24]. The bands around 3402 and 1640 cm^{-1} are more prominent in LW sample, in comparison with the LN and LS samples, due to the hydrophilic character of the LC. These bands could also correspond to absorption bands since they located between 1600 and 1640 cm^{-1} are probably related to the water absorbed in the crystalline phase of the cellulose [25]. These bands are associated with stretching and bending vibrations, respectively.

Furthermore, the presence of the 3402 cm^{-1} band close to the 3405 cm^{-1} band may indicate the presence of cellulose I. The band around 2917 cm^{-1} can be attributed to asymmetric (CH_2) and symmetric (CH_3) stretching vibrations [14,21,25], and according to [26], this band is related to methyl and

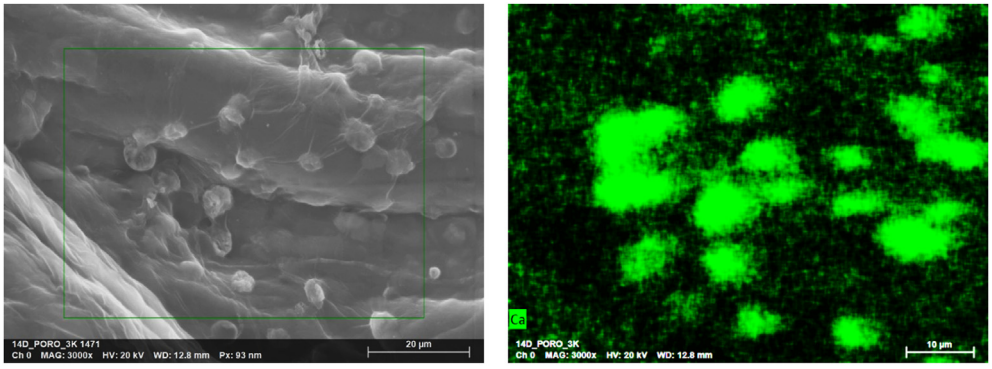

(a) (b)

Fig. 2 – SEM/EDS on (a) the LC natural surface and (b) elemental calcium mapping.

Table 1 – Chemical composition and crystallinity index of *Luffa cylindrica*, natural and treated.

Elements	LN	LW	LS
Chemical composition (wt.%)			
C	54.90	62.94	58.13
O	38.78	35.98	41.21
Ca	3.70	0.62	0.57
K	2.83	0.21	0.09
Others	0.42	0.25	0.00
Crystallinity (%)	69.27	61.39	65.04
Crystallite size (nm)	2.15	2.17	2.34

methylene groups of the cellulose in the fiber. In this work, 2917 cm^{-1} band is associated with the cellulose I structure. No evidence of bands corresponding to cellulose II structure was identified. Bands around 1734 and 1643 cm^{-1} are attributed to the hemicellulose (C=O stretching) and cellulose (OH bending) phases. In this work, it is probable that the band around 1643 cm^{-1} is also associated with the water absorbed because the intensity of this band increased with boiled water treatment. The band around 1047 cm^{-1} is probably more related to C–OH than to the C–C or C–H groups [27] since its increase is more significant in the samples treated with water than in the other samples. After the NaOH treatment, both 1640 and 1047 cm^{-1} bands decrease drastically.

According to Fan et al. [27], the 899 cm^{-1} band is attributed to the nonsymmetric out-of-phase ring. This band is probably associated with the symmetric in-phase stretching mode in the lignin structure [25] and the 897 cm^{-1} band assigned to the amorphous region in the cellulose [28]. On the other hand, the 896 cm^{-1} band is associated with frequency vibration in crystalline cellulose I. It shifts to 893 cm^{-1} in cellulose II when cellulose materials are treated with NaOH/thiourea/urea [29]. It is probable that the 899 cm^{-1} band is more strongly associated with the presence of cellulose I rather than with the lignin structure because the bands related to this structure, around 1579-1519 and 1143 cm^{-1} [25] and the bands 1627 and 1635 cm^{-1} reported by [30], disappeared with the sodium hydroxide treatment.

3.3. XRD – analysis

Fig. 4 shows the XRD spectra of *Luffa cylindrica* untreated and treated with boiled water and sodium hydroxide solution (0.1 mol/L). Likewise, the deconvolution of the X-ray diffraction patterns for natural and treated *Luffa cylindrica*, was performed considering the Gaussian shape function (Eq. (3)) to identify the peaks and overlapping peaks of the spectra. The R-Squared values with the best fit and the iteractions performed were 0.993, 0.986 and 0.985 and 45, 34 and 52 for the LN, LW and LS samples, respectively.

In Fig. 4, it is possible to see all of the most significant peaks corresponding to the amorphous and crystalline phases of the samples at 2θ around 16 and 22°, respectively. Besides, it presents the deconvolution, Fig. 4a, with the baseline subtracted, which identifies the overlapping peaks of the amorphous and crystalline regions at 2θ around 14, 16, 20, 22 and 34°, and the disappearing crystalline phases in LW and LS samples when compared to the LN one. The peaks located around 15.1, 16.4, 22.4, and 34.4°, correspond to the crystal polymorph I of the cellulose [22]. In particular, 15.1 and 16.4° correspond to $(1\bar{1}0)$ and (110) crystallographic planes, respectively. They represent a high rate of amorphous products such as hemicelluloses, lignin and amorphous cellulose. The peaks fitted to 14.27 $(1\bar{1}0)$ and 20.27° (100) by the deconvolution process are associated with cellulose I and cellulose II [27,30,31]. The minimum intensity of the peak at 20.27° could indicate the presence of cellulose II, which agrees with the FTIR results since no bands related to

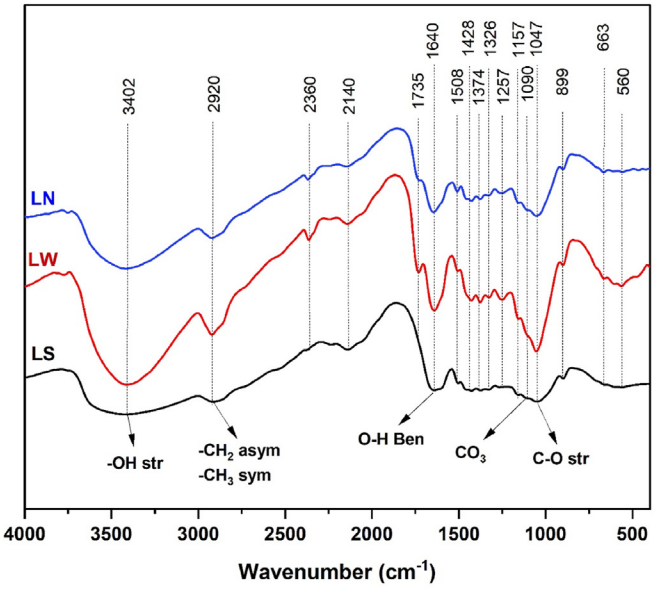

Fig. 3 – FTIR spectra of the *Luffa cylindrica* untreated (LN) and treated with boiled water (LW) and sodium hydroxide (LS) solutions.

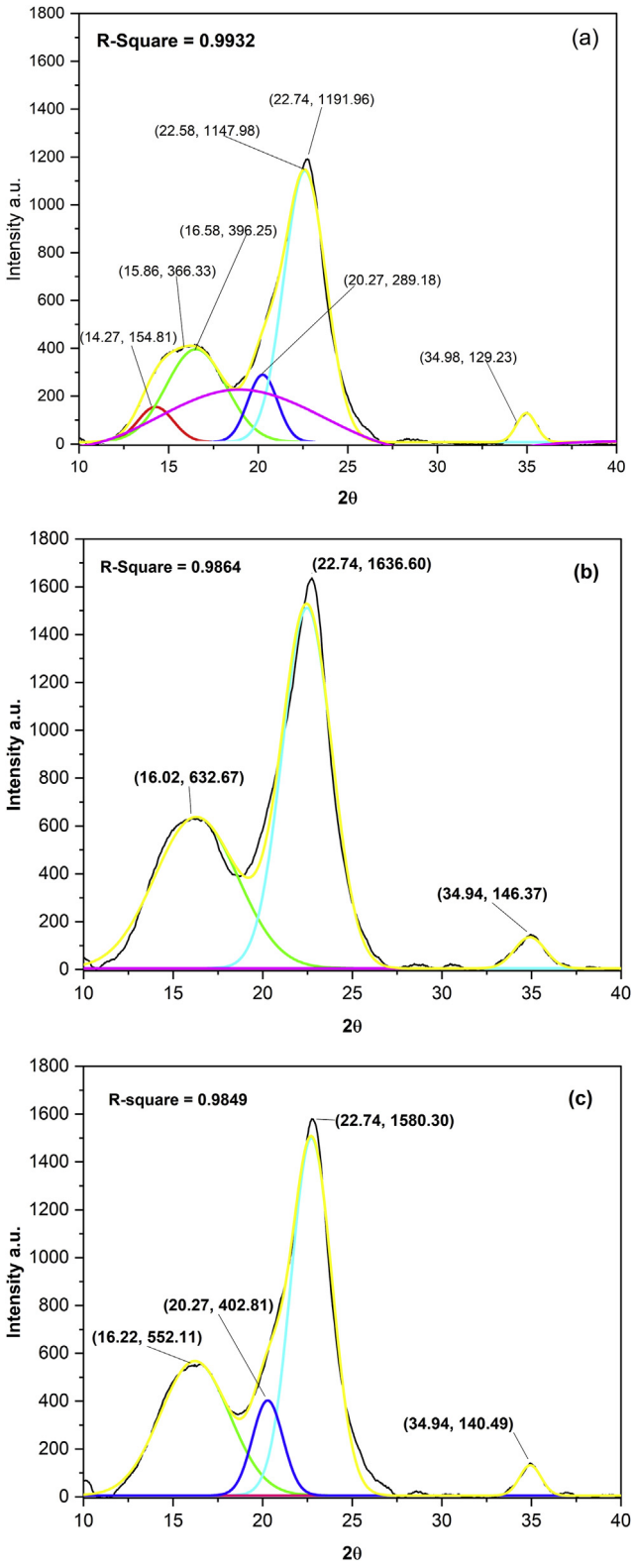

Fig. 4 – XRD spectra of the *Luffa cylindrica* (a) untreated (LN) and treated with (b) boiled water (LW) and (c) sodium hydroxide solution (LS). Curves: black-experimental; yellow – Peaksum; Pink - amorphous cellulose; Cyan, Red, Blue, Green - crystalline cellulose.

the presence of other cellulose types were found, only those related to cellulose I. The other peak, around 34°, is also associated with the cellulose I and the (023) crystallographic plane [22].

Chemical composition, crystallinity index, and crystallite size results are shown in Table 1. It can be seen that the crystallinity indexes are 69.27, 61.39 and 65.04% for LN, LW and LS, respectively. It is possible to verify that the treatment methods carried out produce a decrease in crystallinity. The changes take place in both crystalline and amorphous phases of the cellulose. This reduction may be associated with the removal of the calcium compound and is more pronounced in the LW sample. The LS crystallinity index is higher than that of the LW sample. It can be associated with the total or partial elimination of the hemicellulose and lignin structures by hydrolyzation, which reduces the amorphous region.

Regarding the crystallite size, it is possible to verify that there is a direct relationship between crystallinity and crystallite size for LW and LS samples. Since the LS sample has higher crystallinity, it has a larger crystal size. According to Gong et al. [31], cellulose with lower crystallinity might have a smaller crystallite size. However, in this work, the LN, which has the higher crystallinity of the three samples, has a smaller crystallite size.

4. Conclusions

Comparing the results of the two thermochemical treatments applied, boiled water and sodium hydroxide, it can be concluded that the treatment with sodium hydroxide induced essential alterations in the surface morphology since the smooth surface of the LS sample differs remarkably from the rough and striated appearance of the LN and LW samples. In addition, the treatments produced significant alterations in the structures of the crystalline and amorphous phases of cellulose, lignin, and hemicellulose. Both treatments caused a reduction in the crystallinity index compared to LN fibers, which could be strongly associated with the removal of the calcium compound. Regarding the use of these fibers as fillers in CEB, it is possible to deduce that the amorphous phases, the hemicellulose, and the lignin are directly related to the mechanical performance of the CEB, influencing negatively. Therefore, even when better results were obtained with the LS treatment, perhaps convenient results can also be achieved by varying the water treatment time.

Data availability

The authors confirm that the data supporting the findings of this study are available within the article.

Compliance with ethical standards

All procedures performed in studies do not involve human participants in accordance with the ethical standards of the institutional and/or national research committee and comparable ethical standards.

Declaration of Competing Interest

The authors declare that they have no conflict of interest.

Acknowledgments

The authors are grateful to CONACYT/PROCIENCIA/FEEI/Paraguay for the financial support through the POSG17-53 and BNAC02 programs.

REFERENCES

[1] Pasquini D, De Morais Teixeira E, Da Silva Curvelo A, Belgacem M, Dufresne A. Surface esterification of cellulose fibres: processing and characterization of low-density polyethylene/cellulose fibres composites. Compos Sci Technol 2009;68(1):193. https://hal.archives-ouvertes.fr/hal-00524472/document.

[2] Wang W, Cai Z, Yu J. Study on the chemical modification process of jute fiber. J Eng Fiber Fabr 2008;3(2):1–11. https://journals.sagepub.com/doi/pdf/10.1177/155892500800300203.

[3] Saroya AS, Meena V. Study of mechanical properties of hybrid natural fiber composite. B.Tech. dissertation. Rourkela: National Institute of Technology Rourkela; 2011. http://ethesis.nitrkl.ac.in/2155/1/study_of_mechanical_properties_of_hybrid_natural_fiber_composite.pdf.

[4] Cullen RK, Singh MM, Summerscales J. Characterization of natural fibre reinforcements and composites. J Compos 2013:1–4. https://downloads.hindawi.com/archive/2013/416501.pdf.

[5] Fidelis MEA, Pereira TVC, Gomes OFM, Silva FA, Toledo Filho RD. The effect of fiber morphology on the tensile strength of natural fibers. J Mater Res Technol 2013;2(2):149–57. https://core.ac.uk/download/pdf/82740976.pdf.

[6] Sood M, Dwivedi G. Effect of fiber treatment on flexural properties of natural fiber reinforced composites: a review. Egypt J Petrol 2018;27:775–83. https://doi.org/10.1016/j.ejpe.2017.11.005.

[7] Martínez-Barrera G, Martínez-López M, Martínez-Cruz E. Concreto polimérico reforzado con fibras de luffa. Inf Tecnol 2013;24(4):67–74. https://scielo.conicyt.cl/pdf/infotec/v24n4/art08.pdf.

[8] Dias NA, Xavier MPC, Malaquias NG, Santos EP, da Silva MLCP. Isolamento da celulose de bucha vegetal (*Luffa cylindrica*) via diferentes tratamentos químicos para geração de material de reforço. In: Associação Brasileiro de Engenharia Química, organizer. Proceedings of the XX COBEQ; 2014 Oct 19-22; Florianópolis, Brazil; 2015. http://doi/10.5151/chemeng-cobeq2014-2050-16118-155945.

[9] Tong Y, Zhao S, Ma J, Wang L, Zhang Y, Gao Y, et al. Improving cracking and drying shrinkage properties of cement mortar by adding chemically treated luffa fibres. Construct Build Mater 2014;71:327–33. https://doi.org/10.1016/j.conbuildmat.2014.08.077.

[10] Abdulrahman SA, Aiyejina EE, Paschal UA. Mechanical properties of *Luffa cylindrica* reinforced bio-composite. Int J Curr Res 2015;7(4):14460–4. https://www.journalcra.com/sites/default/files/issue-pdf/8475.pdf.

[11] Colorado HA, Colorado SA, Buitrago-Sierra R. Portland cement with luffa fibers. In: Kriven WM, Wang J, Zhu T, editors. Development in strategic ceramic materials; 2015. p. 104–11. https://doi.org/10.1002/9781119211747.ch9. Ceramic engineering and science proceedings. Chapter 9. Florida, USA.

[12] Mota MKF. Obtenção e caracterização de um compósito de matriz polimérica com carga de bucha vegetal *Luffa cylindrica*. D.Sc. dissertation. Natal, Brasil: Universidade Federal do Rio Grande do Norte; 2016. https://repositorio.ufrn.br/handle/123456789/21147.

[13] Daniel-Mkpume CC, Ugochukwu C, Okonkwo EG, Fayomi OSI, Obiorah SM. Effect of *Luffa cylindrica* fiber and particulate on the mechanical properties of epoxy. Int J Adv Manuf Technol 2019;102:3439–44. https://core.ac.uk/download/pdf/219507454.pdf.

[14] Ad C, Djedid M, Benalia M, Boudaoud A, Elmsellem H, Saffedine FB. Adsorptive removal of nickel (II) using *Luffa cylindrica*: effect of NaCl concentration on equilibrium and kinetic parameters. In: Kallel A, Ksibi M, Ben Dhia H, Khélifi N, editors. Recent advances in environmental science from the euro-mediterranean and surrounding regions. EMCEI 2017. Advances in science, technology & innovation (IEREK interdisciplinary series for sustainable development). Cham: Springer; 2018. https://doi.org/10.1007/978-3-319-70548-4_383.

[15] Anastopoulos I, Pashalidis I. Environmental applications of *Luffa cylindrica*-based adsorbents. J Mol Liq 2020;319(114127):1–9. https://doi.org/10.1016/j.molliq.2020.114127.

[16] Alhijazi M, Safaei B, Zeeshan Q, Asmael M, Eyvazian A, Qin Z. Recent developments in luffa natural fiber composites: review. Sustainability 2020;12(7683):1–25. https://doi.org/10.3390/su12187683.

[17] Kesraoui A, Bouzaabia S, Seffen M. The combination of *Luffa cylindrical* fibers and metal oxides offers a highly performing hybrid fiber material in water decontamination. Environ Sci Pollut Res 2019;26:11524–34. https://doi.org/10.1007/s11356-018-1507-3.

[18] Liatsou I, Christodoulou E, Pashalidis I. Thorium adsorption by oxidized biochar fibres derived from *Luffa cylindrica* sponges. J Radioanal Nucl Chem 2018;317:1065–70. https://doi.org/10.1007/s10967-018-5959-1.

[19] Khadira A, Negarestani M, Mollahosseini A. Sequestration of a non-steroidal anti-inflammatory drug from aquatic media by lignocellulosic material (*Luffa cylindrica*) reinforced with polypyrrole: study of parameters, kinetics, and equilibrium. J Environ Chem Eng 2020;8(3):1–14. https://doi.org/10.1016/j.jece.2020.103734.

[20] Li Y, Zhang M. Mechanical properties of activated carbon fibers. In: Chen JY, editor. Activated carbon fiber and textiles. Amsterdam: Elservier; 2017. p. 167–80. https://doi.org/10.1016/C2014-0-03521-6.

[21] Segal L, Creely JJ, Martin Jr AE, Conrad CM. An empirical method for estimating the degree of crystallinity of native cellulose using the X-ray diffractometer. Textil Res J 1959:786–94. https://doi.org/10.1177/004051755902901003.

[22] Tserki V, Zafeiropoulos NE, Simon F, Panayiotou C. A study of the effect of acetylation and propionylation surface treatments on natural fibres. Composites Part A 2005;36:1110–8. https://doi.org/10.1016/j.compositesa.2005.01.004.

[23] Ghali L, Msahli S, Zidi M, Sakli F. Effect of pre-treatment on luffa fibres on the structural properties. Mater Lett 2009;63:61–3. https://doi.org/10.1016/j.matlet.2008.09.008. 2009.

[24] Fan M, Dai D, Huang B. Fourier transform infrared spectroscopy for natural fibres. In: Salih S, editor. Fourier transform-materials analysis. Intech; 2012. p. 45–68. https://doi.org/10.5772/35482.

[25] Nagarajaganesh B, Muralikannan R. Extraction and characterization of ligno-cellulosic fibers from *Luffa cylindrica* fruit. Int J Polym Anal Char 2016;21(3). https://doi.org/10.1080/1023666X.2016.1146849.

[26] Parida C, Dash S, Pradhan C. FTIR and Raman studies of cellulose fibers of *Luffa cylindrica*. Open J Compos Mater 2015;5:5–10. https://doi.org/10.4236/ojcm.2015.51002.
[27] Chawla KK. Composite materials science and engineering. 3rd ed. New York: Springer-Verlag New York; 2012. https://doi.org/10.1007/978-0-387-74365-3.
[28] Hospodarova V, Singovszka E, Stevulova N. Characterization of cellulosic fibers by FTIR spectroscopy for their further implementation to building materials. Am J Anal Chem 2018;9:303–10. https://doi.org/10.4236/ajac.2018.96023.
[29] Yang YP, Zang Y, Lang YX, Yu MH. Structural ATR-IR analysis of cellulose fibers prepared from a NaOH complex aqueous solution. In: The electrochemical society, organizer. 240th ECS meeting; 2017. https://doi.org/10.1088/1757-899X/213/1/012039. Oct 10-14. Orlando, Florida, USA.
[30] Quinayá DCP, D'almeida JJRM. Nondestructive characterization of epoxy matrix composites reinforced with luffa lignocellulosic fibers. Rev Mater 2017;22(2):1–7. https://doi.org/10.1088/1757-899X/213/1/012039.
[31] Gong J, Li J, Xu J, Xiang Z, Mo L. Research on cellulose nanocrystals produced from cellulose sources with various polymorphs. Royal Soc Chem 2017;7:33486–93. https://doi.org/10.1039/c7ra06222b.